

# RISQ - reduced instruction set quantum computers

Klaus Mølmer and Anders Sørensen

Institute of Physics and Astronomy, University of Aarhus, DK-8000 Århus C, Denmark

November 13, 2018

## Abstract

Candidates for quantum computing which offer only restricted control, *e.g.*, due to lack of access to individual qubits, are not useful for *general purpose* quantum computing. We present concrete proposals for the use of systems with such limitations as RISQ - *reduced instruction set* quantum computers and devices - for simulation of quantum dynamics, for multi-particle entanglement and squeezing of collective spin variables. These tasks are useful in their own right, and they also provide experimental probes for the functioning of quantum gates in pre-mature proto-types of quantum computers.

## 1 Introduction

Notwithstanding dedicated theoretical and experimental efforts, progress in practical implementation of quantum computing is not advancing rapidly. Quantum computing is based on the superposition principle which, when applied to an information carrying system, suggests that parallel processing of a large number of states, *e.g.*, to be identified with inputs to a function, is possible. Only recently it was realized that unitary evolution of superposition states followed by measurements, allowed by quantum theory, provides computational powers, exceeding the one of classical computers [1, 2]. Since then many strategies for practical quantum computing have been investigated. Due to the coincidence of few-qubit quantum computing and ingredients of the advanced field of optimal control [3], already exercised extensively in molecular magnetic resonance spectroscopy, researchers in that field have been able to rapidly implement a number of theoretical quantum computing proposals [4], but the molecular systems are not promising for larger scale computation. Ingredients from the past years' successful experimental control of atoms and single quantized field modes [5, 6], trapped ions [7], donor spin states in solids [8], quantum dots [9] and Josephson junctions [10] have been tailored to yield proposals for single qubit and two-qubit operations, scalable, in principle, to quantum computation with an arbitrary number of qubits.

Experimental research groups now study these proposals, and it is clear that we will see much progress in the coming years, but also that quantum computing is not going to be easy. The development of quantum computers and the progress of our research in quantum computing, is further hampered by the fact that a small quantum computer is of little practical use, and so is a large one which only “gets the answer almost right” (in contrast to one that “gets the correct answer, but only sometimes”).

We suggest in this paper to identify applications of quantum computers with reduced capabilities. We shall use the name RISQ computers (Reduced Instruction Set Quantum computers) for such devices, and we present examples of RISQ computers which may be used to solve quantum problems, much in the spirit of Feynman's proposal for quantum computing [11]. It was suggested by Lloyd [12] that the restriction of physics problems due to locality and symmetries makes such a computer potentially much less demanding to realize in practice than the general purpose quantum computer. Indeed, we shall show that the reduced capabilities of our RISQ systems may just coincide with these physical restrictions, so that they do not present obstacles to “Feynman quantum computing”. We point out that for atoms and ions, entanglement produced by RISQ mechanisms may improve spectroscopic resolution, atomic clocks,

and length and frequency standards. We believe that RISQ ideas will soon lead to operative and useful devices.

We shall focus on practical proposals. In Section 2, we present a scheme for quantum gates and multi-particle entanglement in ion traps, which may be applied for full scale quantum computing, but which may also be applied in a RISQ version without experimental access to individual ions in the trap. In Section 3, we discuss quantum computing with neutral atoms in optical lattices in a RISQ version without access to the individual atoms, useful for simulations of anti-ferromagnetism and for improvement of atomic clocks beyond the fundamental projection noise limit. Section 4 concludes the paper with an optimistic view on quantum information processing as a tool in physics.

## 2 Ion trap quantum computers

### 2.1 General purpose quantum computing in ion traps

At low temperatures trapped ions freeze into a crystal where the Coulomb repulsion among the ions equilibrates the confining force from the trapping potential. The vibrations of the ions are strongly coupled due to the Coulomb interaction, and in the harmonic oscillator approximation they form a set of collective vibrational modes. One may excite one of these modes by tuning a laser to one of the upper or lower sidebands of the ions, *i.e.*, by choosing the frequency of the laser equal to the resonance frequency of an internal transition in an ion plus or minus the vibrational frequency. The laser is then on resonance with an excitation of the internal transition and a simultaneous change in the vibrational motion. This coupling of internal and external degrees of freedom has been extensively used for precise control of the quantum state of trapped ions [7], and in 1995 Cirac and Zoller proposed that the ion trap can be used for quantum computing [13].

In the ion trap quantum computer a qubit is represented by the internal states of an ion. Long lived states, like for instance hyperfine structure states, are preferred. Single qubit rotation and two qubit gates are achieved by focusing a laser on each ion and by exploiting the collective vibrations for interaction between the ions. In the original proposal [13] the system is restricted to the joint motional ground state of the ions. By tuning a laser to a sideband, a vibration is excited if the ion irradiated is in a certain internal state. Upon subsequent laser irradiation of another ion, the internal state of that ion is changed only if the vibrational motion is excited. At the end of the resulting two-qubit gate the vibrational excitation is removed and additional gates may subsequently be implemented.

Under the assumptions of perfect access to the ions and complete absence of decoherence, the trapped ions can be used to compute any mathematical function, and since the ions can be initially set to a superposition of all register states, one simultaneously obtains the evaluation of all function values - the magic parallelism of quantum computing. By electron shelving [14], the state of each qubit can be read out very effectively at the end of the calculation, if one can distinguish fluorescence from the different ions in the trap.

### 2.2 Bichromatic excitation scheme

We now describe our proposal [15] for the efficient production of a two-qubit Hamiltonian like  $\sigma_{y,i}\sigma_{y,j}$ , where the Pauli matrices acting on individual ions  $i$  and  $j$  represent the two-level qubit systems, *e.g.*, with  $|0\rangle_i$  and  $|1\rangle_i$  being the eigenstates of  $\sigma_{z,i}$ . A Hamiltonian proportional with  $\sigma_{y,i}$  provides a rotation between the two states  $|0\rangle_i$  and  $|1\rangle_i$ , and products of such operators provide conditional operations which suffice to build a general purpose quantum computer.

We illuminate the two ions of interest with light of two different frequencies,  $\omega_{1,2} = \omega_{eg} \pm \delta$ , where  $\omega_{eg}$  is the internal state transition frequency, and  $\delta$  is a detuning, not far from the trap frequency  $\nu$ . In Fig. 1, we illustrate the action of such a bichromatic laser field on the state of the two ions of interest. As shown in the figure, the initial and final states  $|ggn\rangle$  and  $|een\rangle$ , separated by  $2\omega_{eg} = \omega_1 + \omega_2$  are resonantly coupled, and so are the degenerate states  $|egn\rangle$  and  $|gen\rangle$ , where the first (second) letter denotes the internal state  $e$  or  $g$  of the  $i^{th}$  ( $j^{th}$ ) ion and  $n$  is the quantum number for the relevant

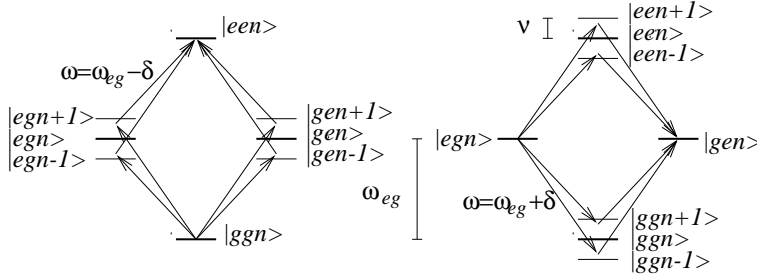


Figure 1: Energy level diagram for two ions with quantized vibrational motion illuminated with bichromatic light. The one photon transitions indicated in the figure are not resonant,  $\delta \neq \nu$ , so only the two-photon transitions shown from  $|ggn\rangle$  to  $|een\rangle$  and from  $|egn\rangle$  to  $|gen\rangle$  are resonant.

vibrational mode of the trap. These resonant couplings lead to an effective Hamiltonian of the form  $\sigma_i^+ \sigma_j^+ + \sigma_i^- \sigma_j^- - \sigma_i^+ \sigma_j^- - \sigma_i^- \sigma_j^+ \propto \sigma_{y,i} \sigma_{y,j}$ .

The restriction of the dynamics to the resonantly coupled states applies in two interesting limits:

### 2.2.1 Weak fields

We can choose the fields so weak and the detuning from the sideband so large that the intermediate states with  $n \pm 1$  photons are not populated in the process. It turns out [15, 16] that as long as the ions remain in the Lamb-Dicke regime, *i.e.*, their spatial excursions are restricted to a small fraction of the wavelength of the exciting radiation, the internal state transition is insensitive to the vibrational quantum number  $n$ . This is due to interference between the interaction paths: The transition via an upper sideband excitation  $|n+1\rangle$ , has a strength of  $n+1$  ( $\sqrt{n+1}$  from raising and  $\sqrt{n+1}$  from lowering the vibrational quantum number), and the transition via  $|n-1\rangle$  yields a factor of  $n$ . Due to opposite signs of the intermediate state energy mismatch, the terms interfere destructively, and the  $n$  dependence disappears from the coupling.

The coherent evolution of the internal atomic state is thus insensitive to the vibrational quantum numbers, and it may be observed with ions in any superposition or mixture of vibrational states, even if the ions exchange vibrational energy with a surrounding reservoir. The control of the thermal motion is of great difficulty in ion trap experiments, and the tolerance to vibrations is a major asset of our bichromatic proposal. In the RISQ section below, we show that the bichromatic gate can also be applied with interesting results without individual access to the ions in the trap, which removes another technical complication for experiments.

### 2.2.2 Strong fields

In the Lamb-Dicke limit with lasers detuned by  $\pm\delta$  our bichromatic interaction Hamiltonian can be written in the interaction picture with respect to the atomic and vibrational Hamiltonian

$$H_{\text{int}} = -\sqrt{2}\eta\Omega J_y [x \cos(\nu - \delta)t + p \sin(\nu - \delta)t], \quad (1)$$

where we have introduced the dimensionless position and momentum operators for the centre-of-mass vibrational mode  $x = \frac{1}{\sqrt{2}}(a + a^\dagger)$  and  $p = \frac{i}{\sqrt{2}}(a^\dagger - a)$ , and where we have introduced the collective internal state observable  $J_y = \frac{\hbar}{2}(\sigma_{y,i} + \sigma_{y,j})$  of the two ions illuminated.  $\Omega$  is the Rabi frequency of the field-atom coupling, and  $\eta$  is the Lamb-Dicke parameter.

The exact propagator for the Hamiltonian (1) can be represented by the ansatz

$$U(t) = e^{-iA(t)J_y^2} e^{-iF(t)J_y x} e^{-iG(t)J_y p}, \quad (2)$$

where the Schrödinger equation  $i\frac{d}{dt}U(t) = HU(t)$  leads to the expressions  $F(t) = -\sqrt{2}\eta\Omega \int_0^t \cos((\nu - \delta)t')dt'$ ,  $G(t) = -\sqrt{2}\eta\Omega \int_0^t \sin((\nu - \delta)t')dt'$ , and  $A(t) = \sqrt{2}\eta\Omega \int_0^t F(t') \sin((\nu - \delta)t')dt'$ .

If  $F(t)$  and  $G(t)$  both vanish after a period  $\tau$ , the propagator reduces to  $U(\tau) = e^{-iA(\tau)J_y^2}$  at this instant, *i.e.*, the vibrational motion is returned to its original state, be it the ground state or any vibrationally excited state, and we are left with an internal state evolution which is *independent* of the external vibrational state [17]. Note that  $(\sigma_y)^2 = 1$  implies that  $J_y^2 = \frac{\hbar^2}{4}(2 + 2\sigma_{y,i}\sigma_{y,j})$ , yielding precisely the interaction that we need. The timing so that  $G(\tau)$  and  $F(\tau)$  vanish allows faster gate operation than in Section 2.2.1, because we tolerate that the internal state is strongly entangled with the vibrational motion in the course of the the gate.

For comparison we show in Fig. 2 the accomplishments of (a) the slow gate and (b) the fast gate evolution. The slow gate is correctly described by Eq. (2), which simplifies because  $F(t)$  and  $G(t)$  are always small. The slow gate may be stopped when  $A(t) \approx -(\Omega\eta)^2 t / (\nu - \delta)$  has acquired its desired value, irrespective of the current, small values of  $F(t)$  and  $G(t)$ . (For illustrational purposes, small but non-zero values of  $F(t)$  and  $G(t)$  were chosen, leading to the small fast oscillations in the figure). To implement the fast gate with a specific value of  $A(\tau)$ , one must choose parameters to fulfill  $F(\tau) = G(\tau) = 0$ . In Fig. 2 (b)  $F(\tau) = G(\tau) = 0$  is achieved at the times  $\tau\nu \approx k \cdot 125$ , where  $k$  is any integer.

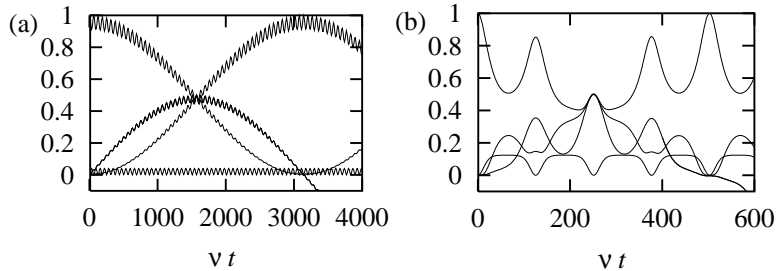


Figure 2: Time evolution of density matrix elements according to (2), with all ions initially in the ground state. (a) Perturbative regime (b) Fast gate. The first curve (counting from above at  $\nu t \approx 1000$  in (a) and  $\nu t \approx 130$  in (b)) represents  $\rho_{gg,gg}$ , the second is the imaginary part of  $\rho_{gg,ee}$ , the third is  $\rho_{ee,ee}$ , and the last curve is the real part of  $\rho_{gg,ee}$ . In (a) the physical parameters are  $\delta = 0.9\nu$ ,  $\eta = 0.1$ , and  $\Omega = 0.1\nu$ . In (b) the physical parameters are  $\delta = 0.95\nu$ ,  $\eta = 0.1$ , and  $\Omega = 0.177\nu$ . The parameters in (b) are chosen such that a maximally entangled state  $\frac{1}{\sqrt{2}}(|gg\rangle - i|ee\rangle)$  is formed at the time  $\nu t \approx 250$ .

## 2.3 RISQ computing in ion traps

### 2.3.1 Feynman computing

The trapped ions or suitable subspaces of states of the ions can be used to represent other physical systems with the same Hilbert space dimension. In the spirit of Feynman's proposal for quantum computing [11], the trapped ions may thus be used for simulation of such other systems.

Let us consider a specific example, where we apply Hamiltonians which are acting identically on all ions, *e.g.*, because laser fields extend over the whole ion cloud rather than being focused down on one or two ions. It follows that a state of the system, which is initially symmetrical under exchange of different ions, will remain symmetrical. A convenient representation of such states is given by the eigenstates of a fictitious total angular momentum,  $|JM\rangle$ , the so-called Dicke states [18]. (Every single two-level ion is generically described by  $2 \times 2$  Pauli spin matrices, and the associated fictitious spin 1/2 add up to a total  $J = N/2$  angular momentum.)

In the Dicke representation,  $N = 2J$  is the total number of ions, and  $M$  counts the number of excited ions,  $N_e = J + M$ . A single resonant laser field, which excites all ions with same amplitude acts as the angular momentum raising operator  $J_+$  on the symmetrical states (and the adjoint lowering operator  $J_-$ ), and effectively it acts as a geometrical rotation of the state vector. Other operators like  $J_y^2$  are of

more interest, in particular if the interaction can be applied to the system in a pulsed fashion to yield the kicked, non-linear rotor, which is a key example of a classically chaotic system.

It is of course not sufficient to make the identification between the states of the relevant system and the states of the trapped ions. We also have to find a way to implement the collective  $J_y^2$  Hamiltonian. In terms of individual raising and lowering operators, it is apparently necessary to introduce interactions among all the particles of the form of the single pair interaction described in the previous subsection. This, however, turns out to be easier than to carry out even a single two-qubit computation: If the trap contains a larger number of ions, which are *all illuminated by the bichromatic light*, any two ions can together resonantly perform the transitions illustrated in Fig. 1, and the Hamiltonian automatically involves the sum over all pairs in the trap. This sum is nothing but the collective operator  $J_y^2$ .

The interest in studying the  $J_y^2$  Hamiltonian was recently stressed by Milburn [17], and it is emphasized by Haake [19] in this issue of J. Mod. Opt. By a simple translation of Haake's arguments for the atom-cavity coupling to the mathematically equivalent trapped ion dynamics, we observe that if ions with more than two levels are used, interaction Hamiltonians of a more complicated structure can be tailored, to simulate, *e.g.*, the SU(2) Lipkin model [19].

### 2.3.2 Multiparticle entanglement

It turns out [20] that the multi-atom collective operator  $J_y^2 = (\frac{\hbar}{2} \sum \sigma_{y,i})^2$  generates a maximally entangled state if it is applied to a whole ensemble of ground state ions,

$$|\Psi\rangle = |gg\dots g\rangle \rightarrow \frac{1}{\sqrt{2}}(e^{i\phi_g}|gg\dots g\rangle + e^{i\phi_e}|ee\dots e\rangle). \quad (3)$$

These states have several very interesting applications both in fundamental physics and technology. They are Schrödinger cat superpositions of states of mesoscopic separation, and they are ideal for spectroscopic investigations.

In current frequency standards the atoms or ions are independent, and when they are interrogated by the same field, the outcome of a measurement fluctuates as the square root of the number of atoms  $N$ . The relative frequency uncertainty in samples with many atoms thus behaves like  $\frac{1}{\sqrt{N}}$ . If the duration of the measurement is shorter than the coherence time of the atomic coherence, which is typically the case in atomic frequency standards, by binding the ions together as in Eq. (3) we are sensitive to the Bohr frequency between  $|gg\dots g\rangle$  and  $|ee\dots e\rangle$  which is proportional to  $N$ , and consequently the frequency uncertainty is proportional to  $\frac{1}{N}$  [21]. If the duration of the frequency measurement exceeds the time scale of internal atomic decoherence  $\tau_{dec}$ , the shorter coherence time  $\tau_{dec}/N$  of the entangled state actually leads to the same resolution for that state and for an uncorrelated ensemble of atoms [22].

The successful implementation of our proposal to produce the state in Eq. (3) with four ions was recently reported by the NIST group in Boulder [23].

## 3 Optical lattice quantum computers

### 3.1 General purpose quantum computing in optical lattices

In Refs. [24, 25] two different methods to perform a coherent evolution of the joint state of pairs of atoms in an optical lattice were proposed. Both methods involve displacement of two optical lattices with respect to each other. Each lattice traps one of the two internal states  $|0\rangle$  and  $|1\rangle$  of the atoms. Initially, the two lattices are on top of each other and the atoms are assumed to be cooled to the vibrational ground state in the lattices. The lattice containing the  $|1\rangle$  component of the wavefunction is now displaced so that if an atom (at the lattice site  $k$ ) is in  $|1\rangle$ , it is transferred to the vicinity of the neighbouring atom (at the lattice site  $k + 1$ ) if this is in  $|0\rangle$ , causing an interaction between the two atoms. See Fig. 3. The atoms interact through controlled collisions or through optically induced dipole-dipole interactions. After the interaction, the lattices are returned to their initial position and the internal states of each atom may

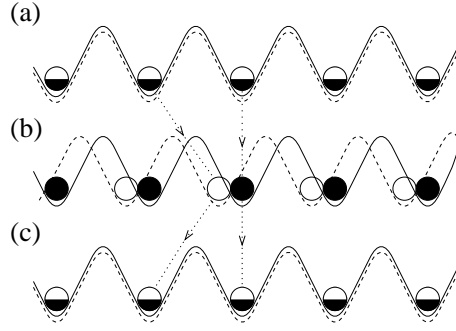


Figure 3: (a) Two overlapping lattices trapping the two internal states  $|0\rangle$  (black circle) and  $|1\rangle$  (white circle). (b) The lattices are displaced so that if an atom is in the  $|1\rangle$  state, it is moved close to the neighbouring atom if this is in  $|0\rangle$  causing an interaction between the two atoms. (c) The lattices are returned to their initial position, where the non-interacting atoms may be driven by external fields.

be subject to single particle unitary evolution. The displacement and the interaction with the neighbour yields a certain phase shift  $\phi$  on the  $|1\rangle_k|0\rangle_{k+1}$  component of the wavefunction, i.e.,

$$\begin{aligned}
 |0\rangle_k|0\rangle_{k+1} &\rightarrow |0\rangle_k|0\rangle_{k+1} & |0\rangle_k|1\rangle_{k+1} &\rightarrow |0\rangle_k|1\rangle_{k+1} \\
 |1\rangle_k|0\rangle_{k+1} &\rightarrow e^{i\phi}|1\rangle_k|0\rangle_{k+1} & |1\rangle_k|1\rangle_{k+1} &\rightarrow |1\rangle_k|1\rangle_{k+1},
 \end{aligned} \tag{4}$$

where  $|a\rangle_k$  ( $a = 0$  or  $1$ ) refers to the state of the atom at the  $k$ 'th lattice site. In [24, 25] it is suggested to build a general purpose quantum computer in an optical lattice based on the two-atom gates in Eq. (4) and single atom control, which is possible by directing a laser beam on each atom.

## 3.2 RISQ computing in optical lattices

Individual access to atoms in an optical lattice is not a realistic demand. The lattice sites are spaced by only a fraction of the optical wave length, and hence focusing of a light beam will not yield single site resolution. One may construct field configurations or magnetic micro-traps with periods larger than optical wavelengths [26] and still use the internal state selective translation and interaction to implement the two-qubit gate. In this section, however, we shall show that there may be interesting possibilities in the optical lattices, despite the lack of access to the individual atoms. We describe how atoms in an optical lattice may be manipulated to simulate spin-spin interactions which are used to describe ferro-magnetism and antiferro-magnetism in condensed matter physics [27]. We also show that with a specific choice of interaction we may generate spin squeezed states [28] which may be used to enhance spectroscopic resolution[29], *e.g.*, in atomic clocks.

### 3.2.1 Feynman computing in an optical lattice

Our two level quantum systems conveniently describe spin  $1/2$  particles with the two states  $|0\rangle_k$  and  $|1\rangle_k$  representing eigenstates of the  $j_{z,k}$ -operator  $j_{z,k}|m\rangle_k = m|m\rangle_k$ ,  $m_z = \pm 1/2$  ( $\hbar = 1$ ). The phase-shifted component of the wavefunction in Eq. (4) can thus be identified with the operator  $(j_{z,k} + 1/2)(j_{z,k+1} - 1/2)$ , and the total evolution composed of the lattice translations and the interaction induced phase shift may be described by the unitary operator  $e^{-iHt}$  with the Hamiltonian  $H = \chi(j_{z,k} + 1/2)(j_{z,k+1} - 1/2)$  and time  $t = \phi/\chi$ . In a filled lattice all atoms are brought into contact with their nearest neighbour according to (4), and the evolution is described by the Hamiltonian  $H = \chi \sum_k (j_{z,k} + 1/2)(j_{z,k+1} - 1/2)$ .

If we neglect boundary terms this Hamiltonian reduces to

$$H_{zz} = \chi \sum_{\langle k,l \rangle} j_{z,k} j_{z,l}, \quad (5)$$

where the sum is over nearest neighbours. By appropriately displacing the lattice we may extend the sum to nearest neighbours in two and three dimensions.  $H_{zz}$  coincides with the Ising-model Hamiltonian [30, 31] introduced to describe ferro-magnetism. Hence, by elementary lattice displacements we perform a quantum simulation of a ferro-magnet (or of an antiferro-magnet depending on the sign of  $\chi$ ). This is an extraordinary example of Feynman quantum computing which is grossly simplified by the locality and the translational invariance of the physical model.

A resonant  $\pi/2$ -pulse acting simultaneously on all atoms rotates the  $j_z$ -operators into  $j_x$ -operators,  $e^{ij_{y,k}\pi/2} j_{z,k} e^{-ij_{y,k}\pi/2} = j_{x,k}$ . Hence, by applying  $\pi/2$ -pulses, in conjunction with the displacement sequence, we turn  $H_{zz}$  into  $H_{xx}$  and  $H_{yy}$ , the second and third term in the more general Heisenberg-model Hamiltonian [32]

$$H_f = \sum_{\langle k,l \rangle} \chi j_{z,k} j_{z,l} + \eta j_{x,k} j_{x,l} + \lambda j_{y,k} j_{y,l}. \quad (6)$$

By adjusting the duration of the interaction with the neighbours we may adjust the coefficients  $\chi$ ,  $\eta$  and  $\lambda$  to any values. We cannot, however, produce  $H_f$  by simply applying  $H_{zz}$  for the desired time  $t$ , followed by  $H_{xx}$  and  $H_{yy}$ , because the different Hamiltonians in Eq. (6) do not commute. Instead we choose short time steps, i.e., small phase shifts  $\phi$  in Eq. (4), and by repeated application of  $H_{zz}$ ,  $H_{xx}$  and  $H_{yy}$ , we approximate the action of  $H_f$  with an error of order  $\phi^2$ .

A host of magnetic phenomena may now be simulated on our optical lattice: Spin waves, solitons, topological excitations, two magnon bound states, etc. Models for magnetic phenomena have interesting thermodynamic behaviour and we propose to carry out calculations for non-vanishing temperature by optically pumping a fraction of the atoms to the  $|1/2\rangle$  state. The randomness of the pumping introduces entropy into the system and produces a micro-canonical [31] realization of a finite temperature.

The results of the simulation may be read out by optical diffraction of light, sensitive to the internal atomic states. Although individual atoms may not be resolved, optical detection may also be used to read out magnetic structures on a spatial scale of a few lattice periods.

For a few atoms the system may be simulated numerically on a classical computer. In Fig. 4 we show the propagation of a spin wave in a one-dimensional string of 15 atoms which are initially in the  $|-1/2\rangle$  state. For illustrational purposes we assume that the central spin is flipped at  $t = 0$ . The Hamiltonian (6) which can be implemented without access to the individual atoms then causes a spin wave to propagate to the left and right.

So far we have assumed that the lattice contains one atom at each lattice site and that all atoms are cooled to the vibrational ground state. The present experimental status in optical lattices is that atoms can be cooled to the vibrational ground-state in 2D [33]. A mean filling factor of unity in 3D is reported in [34], but when at most a single atom is permitted at each lattice site a mean occupation of 0.44 is achieved. The interaction in a partially filled lattice may be described by the Hamiltonian  $H = \sum_{k,l} \chi_{k,l} h_k (j_{z,k} + 1/2) h_l (j_{z,l} - 1/2)$ , where the stochastic variable  $h_k$  is 1 (0) if a lattice site is filled (empty), and where the coupling constants  $\chi_{k,l}$  between atoms  $k$  and  $l$  vanish unless the atoms are brought into contact by the lattice displacements. If we displace the atoms so that  $\chi_{k,l}$  is symmetric in  $k$  and  $l$ , we produce the Hamiltonian  $H = \sum_{k,l} \chi_{k,l} h_k j_{x,k} h_l j_{x,l}$ . This Hamiltonian models magnetism in random structures, and it might shed light on morphology properties, and, *e.g.*, percolation [35].

### 3.2.2 Multi-particle entanglement and spin squeezing

Polarization rotation spectroscopy and high precision atomic fountain clocks are now limited by the  $1/\sqrt{N}$  sensitivity discussed in Sec. 2.3.2 [36, 37]. In [28] it is suggested to produce spin squeezed states which redistribute the uncertainty unevenly between collective spin components like  $J_x$  and  $J_y$ , so that

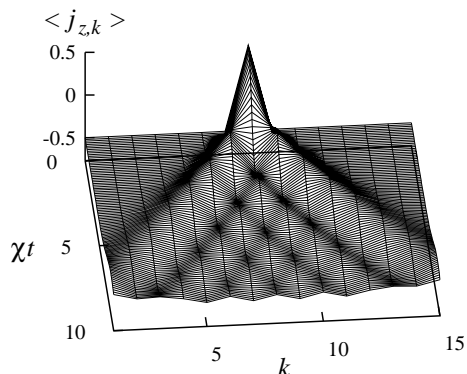


Figure 4: Propagation of a spin wave in a one dimensional string. The central atom is flipped at  $t = 0$ , and repeated application of  $H_{zz}$ ,  $H_{xx}$  and  $H_{yy}$  results in a wave propagating to the left and right. The figure shows the evolution of  $\langle j_{z,k} \rangle$  for all atoms ( $k$ ).

measurements, sensitive to the component with reduced uncertainty, become more precise. Spin squeezing resulting from absorption of non-classical light has been suggested [38] and demonstrated experimentally [39]. Ref. [28] presents an analysis of squeezing obtained from the non-linear couplings  $H = \chi J_x^2$  and  $H = \chi(J_x^2 - J_y^2)$ . The product  $J_x^2$  involves terms  $j_{x,k}j_{x,l}$  for all atoms  $k$  and  $l$ , and this coupling may be produced by displacing the lattices several times so that the  $|1/2\rangle$  component of each atom visits every lattice site and interacts with all other atoms. In a large lattice such multiple displacements are not desirable, they may be too difficult to control precisely, and they take too much time. We shall show, however, that substantial spin-squeezing occurs through interaction with *only a few* nearby atoms.

If each atom visits only its nearest neighbour,  $\chi_{k,l} = \chi\delta_{k+1,l}$ , we find that the mean spin vector is in the negative  $z$  direction and it has the expectation value  $\langle J_z \rangle = -\frac{N}{2} \cos^2(\chi t)$ . The time dependent variance of the spin component  $J_\theta = \cos(\theta)J_x + \sin(\theta)J_y$  with  $\theta = -\pi/4$  is obtained by a lengthy, but straightforward, calculation

$$(\Delta J_{-\pi/4})^2 = \frac{N}{4} \left[ 1 + \frac{1}{4} \sin^2(\chi t) - \sin(\chi t) \right]. \quad (7)$$

Fig. 5 (a) shows the evolution of  $(\Delta J_\theta)^2$  when we visit 1, 2, and 3 neighbours. We assume the same phase shift for all collisions, i.e., all non-vanishing  $\chi_{k,l}$  are identical. The squeezing angle  $\theta = -\pi/4$  is optimal for short times  $\chi t \ll 1$ . For longer times the optimal angle deviates from  $-\pi/4$ , and we plot the variance  $(\Delta J_\theta)^2$  minimized with respect to the angle  $\theta$ . If  $\frac{1}{\sqrt{2}}(e^{-i\theta/2}|1/2\rangle + e^{i\theta/2}| -1/2\rangle)$  is rotated into  $|1/2\rangle$ , subbinomial counting statistics of the  $|1/2\rangle$  population provides an easily accessible experimental signature of squeezing of  $J_\theta$ .

In [29] it is shown that if spectroscopy is performed with  $N$  particles, the reduction in the frequency variance due to squeezing is given by the quantity

$$\xi^2 = \frac{N \langle (\Delta J_\theta)^2 \rangle}{\langle J_z \rangle^2}, \quad (8)$$

and in Fig. 5 (b) we show the minimum value of  $\xi^2$  as a function of the number of neighbours visited. We have performed simulations of squeezing in a partially filled one dimensional lattice. In our model each lattice site contains an atom with a probability  $p$ , and the size of the lattice is adjusted to accommodate 15 atoms. The calculations shown in Fig. 5 (b) demonstrate that considerable squeezing may be achieved by visiting just a few neighbours even in dilute lattices.



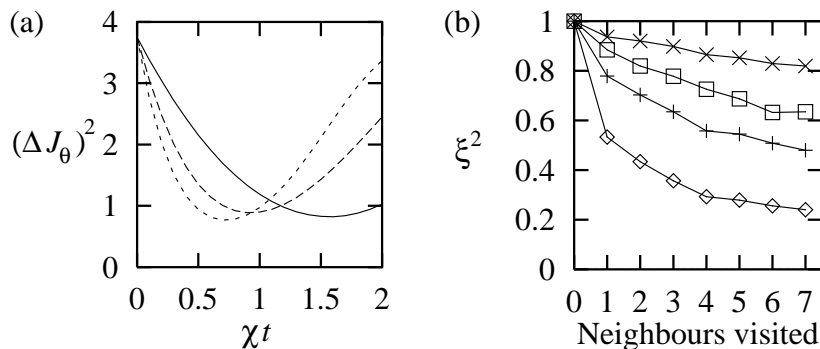


Figure 5: Squeezing in a one-dimensional lattice with 15 atoms. (a) Evolution of  $(\Delta J_\theta)^2$  during interaction with 1, 2, and 3 neighbours (full, dashed, and short dashed line, respectively). (b) Minimum attainable squeezing parameter  $\xi^2$  for filling factors  $p=100\%$  ( $\diamond$ ),  $50\%$  (+),  $25\%$  ( $\square$ ), and  $10\%$  ( $\times$ ) as functions of the number of sites visited.

## 4 Outlook

Our examples with ion trap and optical lattice quantum computers explicitly confirm the assumption [11, 12] that a quantum computer aimed at the solution of a quantum problem may be easier to realize in practice than a general purpose quantum computer, because the desired solution is governed by physical interactions which are constrained, *e.g.*, by locality and symmetries.

The problems addressed here, the kicked non-linear rotor, the Lipkin model, and the Heisenberg model of ferromagnetism and anti-ferromagnetism, almost implement themselves in the quantum computer proposals with trapped ions and atoms. The arguments are general, and one may readily conclude that other proposals for quantum computing offer similar approaches to these models, and that a large variety of quantum physics problems may be implemented much more easily than the more mathematical algorithms of Shor [1] and Grover [2].

If a computation can be carried out with only few operations and in a very short time, the problem of errors is substantially reduced, and it seems realistic that we may soon perform interesting calculations which are really impossible to carry out on a classical computer. Extra optimism derives from the fact that small imprecisions in our manipulation of the system translates into small errors in the value of the physical parameters in the simulated problem, so that, *e.g.* the spin wave in Figure 4, might move at a different speed, but the essential physics is still preserved. The errors are 'normal' and may well be below the precision required, unlike the outcome of a factoring or search algorithm, where a wrong result is useless, and where we have to rely on the exact result to appear with finite probability.

Both trapped ions and atoms in optical lattices are systems which can be used in high precision spectroscopic measurements. We have shown that collective operators for an ensemble of ions or atoms can be squeezed, yielding an improvement of the precision in such measurements. Unlike manufactured systems, like quantum dots or Josephson junctions, given isotopes of ions or atoms are identical, and they can serve as primary time standards. There will hence be a continuing demand to improve experiments on these systems, irrespective of their prospects for full scale quantum computation. Already present atomic clocks are operating at the projection noise limit [37], and multi-particle entanglement and spin-squeezing, in one way or another, will come in handy. Noise reduction derived from multi-particle entanglement provides a macroscopic experimental signature of the microscopic interaction between the atoms, and hence it may help to diagnose gates in an atomic proto-type quantum computer.

Quantum effects are not only subject of experimental investigation. In the hands of experimental physicists wave mechanics is used in SQUIDs and in atom interferometers for sensitive measurements of

fields and inertial effects; electron tunneling is used in the scanning tunneling microscopes; the existence of discrete spectral lines is used for metrology; ... . Quantum information *is* in use in physics, and further developments in quantum information can find applications, ranging from the use of spin-squeezed and Schrödinger cat like states to, *e.g.*, Grover's and Shor's algorithms as methods to distinguish between external influences on a physical system [40] and to effectively estimate values of complex phase factors [41].

We have addressed the use of quantum information as a theorist's computational tool, and in a recent paper [42], Preskill envisions the use of quantum computation for a wide range of many-body problems. A 'symbiosis' between quantum information and these physical problems can even be imagined since, *e.g.*, topological field theories may in turn suggest stronger models and new algorithms for quantum computing [43].

Quantum computing only works, if it can be implemented on a quantum system. There are good chances that RISQ implementations exist for many of the physics problems amenable to quantum computing. To identify such problems, and maybe even some mathematical problems tractable by RISQ, is both an interesting and useful challenge for quantum information theory.

## References

- [1] P. Shor, In *Proceedings of the 35th Annual Symposium on Foundations of Computer Science*, edited by S. Goldwasser (IEE Computer Society, Los Alamos, CA, 1994).
- [2] L. K. Grover, *Phys. Rev. Lett.* **79**, 325 (1997).
- [3] S. Shi and H. Rabitz, *J. Chem. Phys.* **92**, 364 (1990).
- [4] I. L. Chuang, L. M. K. Vandersypen, X. Zhou, D. W. Leung, and S. Lloyd, *Nature* vol. **393**, 143 (1998); I. L. Chuang, N. Gershenfeld, and M. Kubinec, *Phys. Rev. Lett.* **80**, 3408 (1998); J. Jones, M. Mosca, and R. H. Hansen, *Nature* vol **393**, 344 (1998).
- [5] Q. A. Turchette *et al.*, *Phys. Rev. Lett.* **75**, 4710 (1995); X. Maitre *et al.*, *Phys. Rev. Lett.* **79**, 769 (1997).
- [6] P. W. H. Pinkse, *et al.*, *Nature* **404**, 365 (2000); C. J. Hood *et al.*, *Science* **287**, 1447 (2000).
- [7] D. M. Meekhof, *et al.*, *Phys. Rev. Lett.* **76**, 1796 (1996); C. Monroe, *et al.*, *Science* **272**, 1131, (1996).
- [8] B. Kane, *Nature* **393**, 133 (1998).
- [9] A. Imamoglu, *et al.*, *Phys. Rev. Lett.* **83**, 4204 (1999).
- [10] A. Schnirman, *et al.*, *Phys. Rev. Lett.* **79**, 2371 (1997); J. E. Mooij, *et al.*, *Science* **285**, 1036 (1999).
- [11] R. P. Feynman, *Int. J. Theor. Phys.* **21**, 467 (1982).
- [12] S. Lloyd, *Science* **273**, 1072 (1996).
- [13] J. I. Cirac and P. Zoller, *Phys. Rev. Lett.* **74**, 4091 (1995).
- [14] W. Nagourney *et al.*, *Phys. Rev. Lett.* **56**, 2797 (1986), J. C. Bergquist *et al.*, *Phys. Rev. Lett.* **56**, 1699 (1986).
- [15] A. Sørensen and K. Mølmer, *Phys. Rev. Lett.* **82**, 1971 (1999).
- [16] A. Sørensen and K. Mølmer, *Entanglement and quantum computation with ions in thermal motion*, submitted to *Phys. Rev. A*. February 2000, quant-ph/0002024.

- [17] G. Milburn, quant-ph/9908037; the underlying mechanism behind our Eq.(2) was identified by Milburn who applies constant Hamiltonians  $J_y x$ ,  $J_y p$ ,  $-J_y x$  and  $-J_y p$ , and observes that the Baker-Hausdorff relation provides the exponential of the commutator  $[J_y x, J_y p] = i\hbar J_y^2$ .
- [18] R. H. Dicke, Phys. Rev. **93**, 99 (1954).
- [19] Fritz Haake, article in this issue of J. Mod. Opt.
- [20] K. Mølmer and A. Sørensen, Phys. Rev. Lett. **82**, 1835 (1999).
- [21] J. J. Bollinger, *et al.* Phys. Rev. A **54**, 4649 (1996).
- [22] S. F. Huelga, *et al.*, Phys. Rev. Lett. **79**, 3865 (1997).
- [23] C. A. Sackett, Nature **404**, 256 (2000).
- [24] D. Jaksch *et al.*, Phys. Rev. Lett. **82**, 1975 (1999).
- [25] G. K. Brennen *et al.*, Phys. Rev. Lett. **82**, 1060 (1999).
- [26] T. Calarco *et al.*, Phys. Rev. A **61**, 022304 (2000).
- [27] A. Sørensen and K. Mølmer, Phys. Rev. Lett. **83**, 2274 (1999).
- [28] M. Kitagawa and M. Ueda, Phys. Rev. A **47**, 5138 (1993).
- [29] D.J. Wineland *et al.*, Phys. Rev. A **50**, 67 (1994).
- [30] E. Ising, Z. Physik **31**, 253 (1925).
- [31] F. Reif, Fundamentals of statistical and thermal physics, McGraw-Hill (1985).
- [32] N. W. Ashcroft and N. D. Mermin, *Solid State Physics*, Holt-Saunders International Editions, Saunders College, Philadelphia 1976.
- [33] S. E. Hamann *et al.*, Phys. Rev. Lett. **80**, 4149 (1998).
- [34] M. T. DePue *et al.*, Phys. Rev. Lett. **82**, 2262 (1999).
- [35] M. Plischke and B. Bergersen, Equilibrium statistical physics, World Scientific, Singapore (1994).
- [36] J. L. Sørensen *et al.*, Phys. Rev. Lett. **80**, 3487 (1998).
- [37] G. Santarelli *et al.*, Phys. Rev. Lett. **82**, 4619 (1999).
- [38] A. Kuzmich *et al.*, Phys. Rev. Lett. **79**, 4782 (1997).
- [39] J. Hald *et al.*, Phys. Rev. Lett. **83**, 1319 (1999).
- [40] E. Farhi and S. Gutmann, *An analog analogue of a digital quantum computation*, quant-ph/9612026.
- [41] R. B. Griffith and C.-S. Niu, Phys. Rev. Lett. **76**, 3228 (1996).
- [42] J. Preskill, *Quantum information and physics: some future directions*, quant-ph/9904022.
- [43] M. H. Freedman, *et al.*, *Simulation of topological field theories by quantum computers*, quant-ph/0001071.